

IOWA STATE UNIVERSITY

Digital Repository

Ecology, Evolution and Organismal Biology
Publications

Ecology, Evolution and Organismal Biology

8-2016

Scale-Dependent Linkages between Nitrate Isotopes and Denitrification in Surface Soils: Implications for Isotope Measurements and Models

Steven J. Hall

Iowa State University, stevenjh@iastate.edu

Samantha R. Weintraub

University of Utah

David Bowling

University of Utah

Follow this and additional works at: https://lib.dr.iastate.edu/eeob_ag_pubs



Part of the [Biogeochemistry Commons](#), and the [Other Ecology and Evolutionary Biology Commons](#)

The complete bibliographic information for this item can be found at https://lib.dr.iastate.edu/eeob_ag_pubs/214. For information on how to cite this item, please visit <http://lib.dr.iastate.edu/howtocite.html>.

This Article is brought to you for free and open access by the Ecology, Evolution and Organismal Biology at Iowa State University Digital Repository. It has been accepted for inclusion in Ecology, Evolution and Organismal Biology Publications by an authorized administrator of Iowa State University Digital Repository. For more information, please contact digirep@iastate.edu.

Scale-Dependent Linkages between Nitrate Isotopes and Denitrification in Surface Soils: Implications for Isotope Measurements and Models

Abstract

Natural abundance nitrate (NO_3^-) isotopes represent a powerful tool for assessing denitrification, yet the scale and context dependence of relationships between isotopes and denitrification have received little attention, especially in surface soils. We measured the NO_3^- -isotope compositions in soil extractions and lysimeter water from a semi-arid meadow and lawn during snowmelt, along with the denitrification potential, bulk O_2 , and a proxy for anaerobic microsites. Denitrification potential varied by three orders of magnitude and the slope of $\delta^{18}\text{O}/\delta^{15}\text{N}$ in soil-extracted NO_3^- from all samples measured 1.04 ± 0.12 ($R^2 = 0.64$, $p < 0.0001$), consistent with fractionation from denitrification. However, $\delta^{15}\text{N}$ of extracted NO_3^- was often lower than bulk soil $\delta^{15}\text{N}$ (by up to 24 ‰), indicative of fractionation during nitrification that was partially overprinted by denitrification. Mean NO_3^- isotopes in lysimeter water differed from soil extractions by up to 19 ‰ in $\delta^{18}\text{O}$ and 12 ‰ in $\delta^{15}\text{N}$, indicating distinct biogeochemical processing in relatively mobile water versus soil microsites. This implies that NO_3^- isotopes in streams, which are predominantly fed by mobile water, do not fully reflect terrestrial soil N cycling. Relationships between potential denitrification and $\delta^{15}\text{N}$ of extracted NO_3^- showed a strong threshold effect culminating in a null relationship at high denitrification rates. Our observations of (1) competing fractionation from nitrification and denitrification in redox-heterogeneous surface soils, (2) large NO_3^- isotopic differences between relatively immobile and mobile water pools, (3) and the spatial dependence of $\delta^{18}\text{O}/\delta^{15}\text{N}$ relationships suggest caution in using NO_3^- isotopes to infer site or watershed-scale patterns in denitrification.

Keywords

Isotope mass balance model, Mobile water, Nitrification, Redox, Snowmelt

Disciplines

Biogeochemistry | Ecology and Evolutionary Biology | Other Ecology and Evolutionary Biology

Comments

This is a manuscript of an article from *Oecologia* 181 (2016): 1221, doi: [10.1007/s00442-016-3626-1](https://doi.org/10.1007/s00442-016-3626-1). Posted with permission.

**Scale-dependent linkages between nitrate isotopes and denitrification in surface soils:
Implications for isotope measurements and models**

Steven J. Hall^{1,2*}, Samantha R. Weintraub^{1,3}, David R. Bowling^{1,3}

¹Global Change and Sustainability Center, University of Utah

²Department of Ecology, Evolution, and Organismal Biology, Iowa State University

³Department of Geology and Geophysics, University of Utah

⁴Department of Biology, University of Utah

*Contact information for corresponding author:

stevenjh@iastate.edu

608-886-6752

251 Bessey Hall, Iowa State University, Ames, IA 50011

Author contributions: SJH designed the study, SRW and DRB contributed to sample analysis and interpretation, and SJH wrote the paper with contributions from SRW and DRB.

Key words: isotope mass balance model, mobile water, nitrification, redox, snowmelt

Abstract

Natural abundance nitrate (NO_3^-) isotopes represent a powerful tool for assessing denitrification, yet the scale and context-dependence of relationships between isotopes and denitrification have received little attention, especially in surface soils. We measured NO_3^- isotope composition in soil extractions and lysimeter water from a semi-arid meadow and lawn during snowmelt, along with denitrification potential, bulk O_2 , and a proxy for anaerobic microsites. Denitrification potential varied by three orders of magnitude and the slope of $\delta^{18}\text{O}/\delta^{15}\text{N}$ in soil-extracted NO_3^- from all samples measured 1.04 ± 0.12 ($R^2 = 0.64$, $p < 0.0001$), consistent with fractionation from denitrification. However, $\delta^{15}\text{N}$ of extracted NO_3^- was often lower than bulk soil $\delta^{15}\text{N}$ (by up to 24 ‰), indicative of fractionation during nitrification that was partially overprinted by denitrification. Mean NO_3^- isotopes in lysimeter water differed from soil extractions by up to 19 ‰ in $\delta^{18}\text{O}$ and 12 ‰ in $\delta^{15}\text{N}$, indicating distinct biogeochemical processing in relatively mobile water vs. soil microsites. This implies that NO_3^- isotopes in streams, which are predominantly fed by mobile water, do not fully reflect terrestrial soil N cycling. Relationships between potential denitrification and $\delta^{15}\text{N}$ of extracted NO_3^- showed a strong threshold effect culminating in a null relationship at high denitrification rates. Our observations of 1) competing fractionation from nitrification and denitrification in redox-heterogeneous surface soils, 2) large NO_3^- isotopic differences between relatively immobile and mobile water pools, 3) and scale dependence of $\delta^{18}\text{O}/\delta^{15}\text{N}$ relationships suggest caution in using NO_3^- isotopes to infer site or watershed-scale patterns in denitrification.

Introduction

Assessing gaseous nitrogen (N) losses via denitrification from soils and watersheds remains a major challenge in our understanding of ecosystem N dynamics (Groffman, 2012; Kulkarni et al., 2008; Yang et al., 2011). An improved understanding of the spatial and temporal controls on denitrification rates, and their importance in ecosystem N budgets, is critical for addressing problems linked to the cascading impacts of reactive nitrogen in our environment (Galloway et al., 2003). One important method for assessing spatial and temporal patterns in denitrification exploits variation in natural abundance isotopic composition ($\delta^{15}\text{N}$ and $\delta^{18}\text{O}$) of nitrate (NO_3^-) and/or $\delta^{15}\text{N}$ of bulk soils to constrain denitrification losses using $\delta^{15}\text{N}$ mass balance (Bai and Houlton, 2009; Houlton et al., 2006; Houlton and Bai, 2009). Recent studies have expanded on this approach by combining $\delta^{15}\text{N}$ of NO_3^- with $\Delta^{17}\text{O}$, a sensitive tracer of atmospheric NO_3^- (Michalski et al., 2004), to derive gross NO_3^- production (Riha et al., 2014) and denitrification at the watershed scale (Fang et al., 2015). Natural abundance isotopes clearly represent a powerful and minimally invasive tool to assess patterns and controls on denitrification. However, several uncertainties remain with regards to the interpretation of natural abundance NO_3^- isotope measurements in the context of denitrification.

The degree to which NO_3^- stable isotopes can record patterns of denitrification in surface soil horizons (i.e., tens of cm depth), as opposed to deeper subsurface or groundwater environments, has received little attention. It has long been known that significant hot-spots of denitrification can occur in anaerobic microsites in otherwise aerobic soils (Parkin et al., 1987). Houlton et al. (2006) found strong evidence for denitrification in wet surface soils from humid tropical forests using natural abundance N isotopes. In contrast, Fang et al. (2015) used surface soil NO_3^- isotope compositions as inputs to models of watershed-scale denitrification, assuming that nitrification and denitrification were spatially segregated between surface and subsurface

soils, respectively. It remains unclear how surface soil NO_3^- samples might best be collected and interpreted to inform ecosystem-scale isotope models and our broader understanding of denitrification.

Different types of samples, such as soil salt extractions or soil water samples, could differ substantially in their capacity to record NO_3^- isotope effects from denitrification due to differences in water residence time and spatial distribution in the soil. Water has a continuum of mobility in soil according to physical and chemical interactions with soil constituents, which can be quantified according to water potential. Soil extractions capture most of the inorganic nitrogen (including N interacting electrostatically with soil exchange sites) in a sampled soil volume, whereas water collected in vadose zone lysimeters under minimal applied tension may reflect N in comparatively mobile water pools that have a shorter residence time in the soil matrix. Water pools associated with soil mineral and organic surfaces, i.e. less mobile pools, often differ greatly in H_2O isotope composition relative to highly mobile water in soil macropores, reflecting differences in water pool transit time and thus their capacity to record terrestrial biophysical processes (Evaristo et al., 2015; Good et al., 2015). We hypothesize that these water pools might also differ in their capacity to record N biogeochemical processing via stable isotopes. Both soil extractions and lysimeter water collected under various tensions have been used in ecosystem-scale studies involving NO_3^- isotopes, but they have seldom been directly compared. Perhaps even more importantly, differences in NO_3^- stable isotopes among samples have not typically been compared with canonical indices of denitrification, such as potential denitrification enzyme activity.

Comparisons of NO_3^- isotope composition with measured potential denitrification activities could help address possible ambiguities in isotope interpretation. The use of NO_3^-

90 isotopes to infer the occurrence of denitrification relies on kinetic fractionation from denitrifying
91 bacteria, which increases the $\delta^{15}\text{N}$ and $\delta^{18}\text{O}$ of residual NO_3^- (Mariotti et al., 1981). Linear
92 relationships between $\delta^{18}\text{O}$ and $\delta^{15}\text{N}$ of NO_3^- with slopes between 0.5 and 1 are assumed to
93 reflect kinetic fractionation by denitrifiers, a relationship that appears to hold across soils,
94 groundwater, and aquatic ecosystems (Cohen et al., 2012; Granger et al., 2008; Houlton et al.,
95 2006; Lehmann et al., 2003; Sigman et al., 2005). This assumption is plausible given that
96 assimilatory N fractionation by plants and microbes, another explanation for NO_3^- isotope
97 enrichment, is typically minor in N-limited ecosystems (Evans, 2001; Granger et al., 2010).
98 However, co-occurring fractionation from other N-cycling processes, such as nitrification
99 (Mariotti et al., 1981), or N inputs with differing isotope composition, could potentially obscure
100 isotope enrichment from denitrification.

101 In surface soils with heterogeneous O_2 availability, nitrification (an aerobic process) and
102 denitrification (an anaerobic process) can potentially co-occur. In open systems, nitrifying
103 bacteria tend to decrease the $\delta^{15}\text{N}$ of soil NO_3^- relative to NH_4^+ by 14 – 38 ‰ (Casciotti et al.,
104 2003; Mariotti et al., 1981). Open-system fractionation by denitrifying bacteria spans a similar
105 range, increasing $\delta^{15}\text{N}$ of the residual NO_3^- pool between 5 and 29 ‰ (Granger et al., 2008;
106 Mariotti et al., 1981). In cases where NH_4^+ or NO_3^- are fully consumed in soil microsites (i.e.,
107 closed systems), it is also possible that fractionation is partially or not at all expressed during
108 either nitrification or denitrification (Kendall et al., 2007). However, even in cases where
109 fractionation from nitrification and denitrification *are* both expressed at the microsite (ie, μm)
110 scale, it is possible that their effects could be mutually obscured over larger spatial scales (ie,
111 cm) characteristic of soil samples due to their opposite effects on $\delta^{15}\text{N}$ of NO_3^- . This situation
112 potentially creates a challenge for interpretation by obscuring the original isotope composition of

NO₃⁻ inputs, a necessary parameter for quantitative isotope models (e.g. Fang et al., 2015), and diluting the pool of δ¹⁵N-enriched NO₃⁻ that is typically used to indicate the presence of denitrification (Billy et al., 2010; Houlton et al., 2006; Wexler et al., 2014). Comparing traditional indices of denitrification and related biogeochemical parameters with NO₃⁻ isotopes could help to decipher if this isotopically “cryptic” denitrification is important in surface soil environments.

Combining measurements of δ¹⁵N and δ¹⁸O of NO₃⁻ with δ¹⁵N of N sources and δ¹⁸O of soil water could also assist in identifying the occurrence of denitrification in surface soils. The δ¹⁵N of nitrified NO₃⁻ depends both on δ¹⁵N of NH₄⁺ sources and the extent of fractionation during nitrification. Ammonium typically reflects the δ¹⁵N of plant litter, soil organic matter (SOM), or fertilizer from which it is derived, with minimal (~1 ‰) fractionation (Kendall et al., 2007). Atmospheric deposition is another potentially important NH₄⁺ source. A representative range of δ¹⁵N in these NH₄⁺ sources that is specifically applicable to the present study is indicated by the vertical shaded rectangle in Fig 1a. Nitrification of NH₄⁺ fractionates δ¹⁵N substantially in open systems (Casciotti et al., 2003; Mariotti et al., 1981), with potential values indicated by the “nitrification” vertical shaded rectangle in Fig. 1a. Nitrification also imparts a characteristic δ¹⁸O composition to NO₃⁻. Oxygen in nitrified NO₃⁻ is dominantly (ie, ≥ 2/3) derived from soil water, with a variable contribution from atmospheric O₂ (23.5 ‰) that depends on the degree of in-situ O exchange with water (Kool et al., 2011; Mayer et al., 2001). This range is indicated by the nitrification box in Fig. 1a. Subsequent denitrification of this NO₃⁻ pool would presumably be reflected by ~1:1 increases in δ¹⁵N and δ¹⁸O of nitrified NO₃⁻ (indicated by the denitrification arrow in Fig. 1a) which could ultimately return δ¹⁵N of NO₃⁻ to values similar or

greater than the ecosystem N sources (Fig. 1a). However, $\delta^{18}\text{O}$ of NO_3^- would then remain substantially elevated relative to $\delta^{18}\text{O}$ of soil H_2O , inconsistent with NO_3^- derived from nitrification. Mixing of soil NO_3^- with atmospheric inputs is another important consideration. Atmospheric NO_3^- has very high $\delta^{18}\text{O}$ (i.e., 60 – 80 ‰) as a consequence of atmospheric oxidative processes (Kendall et al., 2007), which could also increase $\delta^{18}\text{O}$ of soil NO_3^- relative to the products of nitrification, as indicated by the vertical mixing arrow in Fig. 1a.

To assess relationships between NO_3^- stable isotope composition and microsite-scale denitrification in surface soils, we designed a study involving two nearby sites (a riparian meadow and a managed urban lawn) in a semi-arid montane ecosystem where denitrification likely represents an important fate of N during spring snowmelt. In temperate ecosystems with a seasonal snowpack, snowmelt often represents a period of maximum soil moisture and potential N loss, when soil biogeochemical processes are especially important in attenuating N inputs to streams (Brooks and Williams, 1999; Zak et al., 1990). Our sites provided a natural gradient in denitrification potential, allowing us to assess their relationship with NO_3^- isotopes while maintaining similar climate and soil physical/chemical characteristics. Importantly, these sites also had similar surface soil (0 – 15 cm) NH_4^+ pools, similar plant litter $\delta^{15}\text{N}$, and relatively similar bulk soil $\delta^{15}\text{N}$ (within 1.5 ‰), implying that the initial $\delta^{15}\text{N}$ of NH_4^+ and NO_3^- pools produced by mineralization and nitrification were also likely to be similar between sites.

2. Methods

We sampled soils from two sites in the Red Butte Creek watershed in Salt Lake City, Utah: a natural riparian meadow with herbaceous vegetation (Dawson and Ehleringer, 1991) and a managed lawn on the University of Utah campus. Both sites received $> 4 \text{ kg N ha}^{-1} \text{ y}^{-1}$ in

atmospheric deposition (Hall et al., in review, JGR-Biogeosciences). The lawn received ~ 100 kg ha⁻¹ y⁻¹ of fertilizer N as a urea blend (32 – 5 – 7 ratio of N, P and K) applied during late spring, and ammonium sulfate (20 – 0 – 0) applied during October. Fertilizer was obtained from Intermountain Farmers Association (Salt Lake City, UT). Soils were sampled following spring snowmelt (Feb and Mar 2014 at the lawn and meadow, respectively), approximately five months after the last fertilizer application to the lawn. Snowmelt typically represents the period of maximum soil moisture in semi-arid montane ecosystems.

The meadow soil was a loamy Mollisol with a predominant rooting depth above 35 cm, and the lawn soil was a sandy loam Inceptisol derived from local alluvium added on top of rocks. Bulk density and pH were similar between sites (Table 1). We sampled the meadow at depths of 0 – 5, 5 – 15, and 15 – 35 cm with a 6-cm diameter auger (n = 9 for each depth); the lawn could only be sampled to 15 cm due to an impenetrable rock layer (n = 12 for each depth). Tension lysimeters (Prenart Super Quartz, Denmark) were installed at 15 and 35 cm in the lawn and meadow, respectively, at the bottom of the main rooting zone at each site. Lysimeters were installed approximately five months prior to sampling for this study. Lysimeter water was sampled by applying a vacuum of -28 kPa relative to ambient pressure (86 kPa). This sampling pressure was chosen because its absolute value is similar to but less than field capacity, typically defined as -30 kPa for loamy soils (Schaetzl and Anderson, 2005). Field capacity is an estimate of residual soil water remaining after macropores have drained. Thus, our lysimeters captured water at potentials above field capacity, or a comparatively “mobile” water pool. Others have used tension lysimeters to sample soil water under much more negative water potential (-70 kPa) than we used here, but still judged these samples to reflect water capable of significant advection (Castellano et al., 2013). We stress that the concepts of “mobile” and “immobile” water do not

represent a dichotomy but rather an operationally defined continuum. Because our lysimeters were sampled under tension, they contain some fraction of soil-associated water differing in composition from water that instantaneously drains through soils during melt or precipitation events (Landon et al., 1999). Our operational separation between more and less mobile water pools, respectively sampled in lysimeters and soil extractions, is thus conservative. Water samples were collected throughout the period of snowmelt (total n = 186; Jan – April 2014).

Oxygen (O₂) sensors (Apogee Instruments, Logan, Utah) were installed at depths of 10 cm in 4.8 cm diameter polyvinylchloride pipes with sealed caps (equilibration chambers), where the bottom lip of the chamber was pressed into undisturbed soil (Hall et al., 2013). Soil O₂ content was recorded on a datalogger at 15-minute intervals. Here, we report O₂ during the period of NO₃⁻ sample collection. All of the above measurements were made in the context of a snow removal experiment at each site (Hall et al., 2016a), but given the absence of treatment effects on any biogeochemical response variable, we do not report treatment identities for ease of interpretation. Precipitation was collected on an event basis during the study period for analysis of NO₃⁻ and NH₄⁺ concentrations and isotope composition. Lysimeter and precipitation samples were filtered through pre-combusted and rinsed Whatman GF/F filters and frozen until analysis by ion chromatography.

We measured potential denitrification rates in shaken slurries of soil samples within 24 hours of sampling using the acetylene inhibition method (Groffman et al., 1999), using an incubation temperature of 4 °C to approximate field conditions and 25 °C to facilitate comparisons with other studies. Potential denitrification rates are an appropriate metric to compare with the isotope composition of NO₃⁻ pools because they are tightly linked to the abundance of bacterial denitrification functional genes, which integrate recent process activity in

the soil environment (Petersen et al., 2012). Soil subsamples were extracted in 2M potassium chloride (KCl) solutions for analysis of NH_4^+ and NO_3^- concentrations and isotope composition. We measured $\delta^{15}\text{N}$ and $\delta^{18}\text{O}$ of NO_3^- in soil extractions ($n = 50$), lysimeter water samples ($n = 31$), and precipitation samples ($n = 8$) using *Pseudomonas aureofaciens* and the denitrifier method (Bell and Sickman, 2014; Casciotti et al., 2002) to generate N_2O for analysis by isotope ratio mass spectrometry at the Stable Isotope Ratio Facility for Environmental Research at the University of Utah. When analyzing the soil extractions using the denitrifier method, we corrected for the presence of trace NO_3^- in KCl and any physiological effects on the denitrifying bacteria by analyzing reference materials prepared in the same matrix (Bell and Sickman, 2014). Samples were normalized to δ notation, relative to atmospheric N_2 for N and VSMOW for O, using a combination of the international NO_3^- reference materials USGS 34, 35 and 32. Precision and accuracy were 0.6 ‰ and 0.7 ‰ (respectively) for $\delta^{15}\text{N}$, and 0.6 ‰ and 0.3 ‰ (respectively) for $\delta^{18}\text{O}$, assessed by repeated analysis of IAEANO3 (for $\delta^{15}\text{N}$) and USGS 32 (for $\delta^{18}\text{O}$) treated as unknowns. Sample reproducibility was 0.3 ‰, based on duplicate analyses of 1/8 of the samples. To characterize $\delta^{15}\text{N}$ of fertilizer inputs to the lawn, three subsamples were analyzed from each of two production batches of each fertilizer type (ammonium sulfate and urea). Bulk soil $\delta^{15}\text{N}$ from each site and sampled depth increment, and surface litter ($n = 9$ plots per site), were analyzed on samples dried at 60 °C. Soil and fertilizer $\delta^{15}\text{N}$ were measured via combustion on an elemental analyzer coupled to an isotope ratio mass spectrometer (Thermo MAT 253, Waltham MA). A subset of lysimeter water samples from the meadow site ($n = 17$) was analyzed for $\delta^{18}\text{O}$ of H_2O by isotope ratio infrared spectroscopy (Picarro L-2130i, Santa Clara CA).

A subset of precipitation samples ($n = 15$) was analyzed for $\delta^{15}\text{N}$ of NH_4^+ using a modified NH_3 diffusion method (Holmes et al., 1998). Briefly, 30 ml of sample was added to a

60 ml HDPE bottle with 1.5 g sodium chloride. A glass-fiber filter acidified with 30 μ l of 4M phosphoric acid was pressed between Teflon tape and added to the bottle. Magnesium oxide (90 mg) was added to volatilize NH_3 , and the bottle was immediately capped and incubated for 7 days on an orbital shaker/incubator at 40 °C to allow NH_3 to be completely trapped as NH_4^+ on the acidified filter. Filters were analyzed for $\delta^{15}\text{N}$ (precision < 0.2‰) by combustion as described above. Analysis of ammonium sulfate solutions with known $\delta^{15}\text{N}$ values verified a lack of fractionation during diffusion.

Soil subsamples were also extracted in the field immediately after sampling with 0.5 M hydrochloric acid for analysis of reduced and oxidized iron (Fe(II) and Fe(III), respectively) as a redox indicator (Hall et al., 2013). The presence of Fe(II) implies the presence of anaerobic microsites where dissimilatory Fe reduction exceeds Fe(II) oxidation by O_2 . The ratio of Fe(II)/Fe_{HCl} reflects the proportion of HCl-extractable Fe that has been reduced, facilitating comparisons among sites that may differ in total HCl-extractable Fe content (Hall et al., 2015). Thermodynamic principles imply that NO_3^- should have been consumed via denitrification in microsites where Fe(II) is present (Chapelle et al., 1995).

We analyzed linear relationships between $\delta^{15}\text{N}$ and $\delta^{18}\text{O}$ of NO_3^- both within and among sites and for each separate sample type (soil extractions vs. lysimeter water) using ANCOVA. Mean differences in $\delta^{15}\text{N}$ and $\delta^{18}\text{O}$ composition among sites were assessed using MANOVA (ie, ANOVA testing two response variables simultaneously). Differences in other response variables among sites were assessed with ANOVA. Relationships between $\delta^{15}\text{N}$ of NO_3^- and potential denitrification and Fe(II)/Fe_{HCl} were highly non-linear, so we fit trends with a two-component piecewise linear regression using the SiZer package in R (Sonderegger 2012).

Results

While both sites typically had near-atmospheric O₂ concentrations in the bulk soil throughout the period of measurement, they also showed evidence of redox heterogeneity and the presence of reducing conditions in soil microsites as reflected by Fe(II)/Fe_{HCl} ratios (Table 1). The lawn had much higher Fe(II)/Fe_{HCl} relative to the meadow ($p < 0.0001$), coinciding with increased potential denitrification rates. Denitrification potential was 16-fold greater in lawn soils at 4 °C ($p < 0.0001$) and 6-fold greater at 25 °C ($p < 0.001$; Table 1) when considering all depth increments combined. Nitrate concentrations in soil extractions were generally similar between sites, although lysimeter NO₃⁻ was significantly greater in the lawn (Table 1).

Bulk soil $\delta^{15}\text{N}$ was similar between sites in 0 – 5 cm soil, but was slightly (1.5 ‰) and significantly ($p < 0.0001$) greater in lawn 5 – 15 cm soil (Table 1). Despite the fact that NH₄⁺ concentrations significantly differed between sites at a given depth increment ($p < 0.001$), total KCl extractable NH₄⁺ mass to 15 cm was similar between the meadow and lawn, measuring 0.056 (0.013) and 0.044 (0.003) kg NH₄⁺-N ha⁻¹, respectively. At the lawn, comparison of the KCl extractable NH₄⁺ pool with annual NH₄⁺ fertilizer inputs indicated that > 99.9 % of the previous year fertilizer application was assimilated, or otherwise transformed or exported, prior to measurement. Surface litter $\delta^{15}\text{N}$ was also similar between the meadow (-0.5 ± 0.1 ‰) and lawn (0.1 ± 0.4 ‰). Fertilizer $\delta^{15}\text{N}$ was highly consistent within and between production batches and was relatively similar between the two fertilizer types applied here. Two separate batches of ammonium sulfate $\delta^{15}\text{N}$ measured -0.9 ± 0.2 and -1.0 ± 0.3 ‰, and the urea blend $\delta^{15}\text{N}$ was -1.7 ± 0.1 and -1.6 ± 0.3 ‰. Values of $\delta^{15}\text{N}$ of NH₄⁺ in bulk atmospheric deposition measured -1.2 ± 1.5 ‰, similar to fertilizer.

Trends in $\delta^{18}\text{O}$ and $\delta^{15}\text{N}$ of NO_3^- in soil extractions from both sites considered together were consistent with linear isotopic effects from denitrification of NO_3^- sources with similar initial isotope values, reflected by a slope of 1.04 ± 0.12 ($R^2 = 0.64$, $p < 0.0001$; Fig. 1b). The slope of this relationship did not differ significantly between sites. However, the relationship between $\delta^{18}\text{O}$ and $\delta^{15}\text{N}$ was insignificant when assessing samples from the lawn alone (slope = 0.62 , $R^2 = 0.10$, $p = 0.21$) and was much stronger in the meadow (slope = 0.72 ± 0.13 , $p < 0.0001$, $R^2 = 0.55$). Nevertheless, the lawn extractions had significantly greater (more enriched) NO_3^- $\delta^{18}\text{O}$ and $\delta^{15}\text{N}$ values than the meadow ($p < 0.0001$; Fig. 1b, Table 2). Nitrate $\delta^{15}\text{N}$ in soil extractions also had a weakly significant site by depth interaction ($p = 0.02$), where values did not differ by depth in the lawn but were significantly greater in meadow 0 – 5 cm samples than the deeper samples.

In contrast to the soil extractions, $\delta^{18}\text{O}$ and $\delta^{15}\text{N}$ of lysimeter NO_3^- were not significantly correlated, and lysimeter NO_3^- isotope composition did not differ between sites (Fig. 1b, Table 2). Furthermore, lysimeter samples significantly differed in NO_3^- isotope composition when compared with soil extractions from the same site (MANOVA, $p < 0.0001$; Fig. 1b). Values of $\delta^{18}\text{O}$ in precipitation NO_3^- (81.9 ± 4.0 ‰) were substantially greater than any of the soil extractions or soil lysimeter samples, while $\delta^{15}\text{N}$ of precipitation NO_3^- (2.3 ± 0.7 ‰; Table 2) fell within the bounds of soil extractions and lysimeter samples. Neither the soil extractions nor lysimeter samples displayed significant relationships between NO_3^- isotope composition and NO_3^- concentrations (data not shown).

Nitrate $\delta^{15}\text{N}$ showed distinct trends with potential denitrification and $\text{Fe(II)/Fe}_{\text{HCl}}$ at both sites: significant linear trends at the meadow ($p < 0.001$ and 0.03 , respectively), but no

relationship at the lawn. Combined, these data suggested significant threshold relationships between $\delta^{15}\text{N}$, potential denitrification, and $\text{Fe(II)}/\text{Fe}_{\text{HCl}}$ as determined by piecewise linear regressions (Fig. 2). Nitrate $\delta^{15}\text{N}$ initially increased sharply with potential denitrification (slope = 0.75, between 0.10 and 0.90 with 95 % confidence) and $\text{Fe(II)}/\text{Fe}_{\text{HCl}}$ (slope = 170, between 60 and 550 with 95 % confidence), but subsequently plateaued to slopes indistinguishable from zero for both response variables (Fig. 2).

Discussion

We found evidence that denitrification was likely occurring during snowmelt in surface soil horizons at both sites, as reflected by substantial rates of potential denitrification activity combined with the presence of anaerobic microsites as reflected by $\text{Fe(II)}/\text{Fe}_{\text{HCl}}$. Although high potential denitrification rates indicate the presence of denitrifying organisms, they do not definitively indicate when denitrification may have occurred. In these ecosystems, increased soil moisture during snowmelt likely generated anaerobic microsites that promoted denitrification, given that very low soil moisture (< 10 % by volume) prevailed for several months prior at each site until snowmelt began (Hall et al., 2016a). The importance of denitrification in cold soils during snowmelt has been well established in other studies (Brooks et al., 2011), and our measured potential denitrification activities at 25 °C were similar to rates from wetland and riparian soils in other studies (Roach and Grimm, 2011). Yet, different NO_3^- samples (soil extractions vs. lysimeter water) and sites (the lawn and meadow) varied dramatically in their relationships between $\delta^{15}\text{N}$ and $\delta^{18}\text{O}$ and proxies for denitrification.

Trends in NO_3^- isotopes in soil extractions and proxies for denitrification

Plotting $\delta^{18}\text{O}$ vs. $\delta^{15}\text{N}$ of NO_3^- in soil extractions from both sites yielded a slope similar to one, consistent with the upper bound of slopes invoked as evidence for denitrification in previous field studies in terrestrial, groundwater, and marine environments (Cohen et al., 2012; Houlton et al., 2006; Lehmann et al., 2003; Sigman et al., 2005), and similar to laboratory experiments with denitrifying bacteria (Granger et al., 2008). However, $\delta^{15}\text{N}$ of NO_3^- remained lower than bulk soil N in most samples, despite the fact that denitrification had demonstrably occurred. These trends are consistent with a large initial isotope fractionation from nitrification (Casciotti et al., 2003) which was subsequently impacted by denitrification to a variable extent among samples. A large fractionation from nitrification is consistent with the observed presence of excess NH_4^+ at both sites relative to NO_3^- (Table 1), and comparatively slow enzymatic catalysis in cold soils following snowmelt. A large isotopic effect of nitrification was also recently observed in New Zealand pasture soils during winter (Wells et al., 2015).

Our interpretations of $\delta^{15}\text{N}$ of NO_3^- are enhanced by considering potential variation in $\delta^{15}\text{N}$ of the NH_4^+ from which NO_3^- is derived. We argue that there were not likely to be systematic differences in $\delta^{15}\text{N}$ of NH_4^+ between sites, according to the following reasoning. The major potential sources of NH_4^+ at these sites during the period of sampling include mineralization of litter and SOM, residual fertilizer at the lawn, and atmospheric deposition. Most importantly for our study, these potential NH_4^+ sources had relatively similar $\delta^{15}\text{N}$ composition in comparison with the observed variation in $\delta^{15}\text{N}$ of NO_3^- , and tended to be similar between sites. First, mineralized NH_4^+ has similar $\delta^{15}\text{N}$ (± 1 ‰) relative to the organic matter (e.g., litter or SOM) from which it was derived (Kendall et al., 2007), and differences in litter and SOM $\delta^{15}\text{N}$ pools between the two sites were small (< 0.5 and 1.5 ‰, respectively). Multiple litter and SOM pools mineralize NH_4^+ at different rates, so it is likely that the measured

differences between litter and bulk soil $\delta^{15}\text{N}$ (-0.5 to 5.8 ‰) approximate the range of variation in $\delta^{15}\text{N}$ of mineralized NH_4^+ at these sites. Mean fertilizer (-0.9 – 0.1 ‰) and atmospheric deposition (2.3 ‰) $\delta^{15}\text{N}$ fell close to or within this range. We suggest that mineralization of litter and SOM (as opposed to fertilizer) were especially important sources of NH_4^+ in both the meadow and the lawn during the period of sampling. This interpretation was supported by 1) the fact that total extractable NH_4^+ stocks were *equivalent* between lawn and meadow despite fertilization; 2) the very small extractable pool of NH_4^+ relative to annual fertilizer inputs, indicative of rapid cycling of mineral N where > 99.9 % of fertilizer N inputs were assimilated or lost via gaseous or leaching pathways prior to sampling; 3) the fact that six months had elapsed since fertilizer application, providing ample opportunity for assimilation or other transformations. Even if residual fertilizer did represent a significant component of soil NH_4^+ , it is unlikely to lead to substantial differences in $\delta^{15}\text{N}$ of NH_4^+ between sites given that fertilizer $\delta^{15}\text{N}$ was very similar to litter $\delta^{15}\text{N}$ at both sites.

Secondly, it is plausible to assume that initial $\delta^{15}\text{N}$ values of nitrified NO_3^- may also have been similar between sites and depths. This assumption is reasonable given overall similarities in NH_4^+ concentrations, bulk soil N concentration and $\delta^{15}\text{N}$, microbial biomass N, pH, bulk density, and climate between the lawn and meadow (Hall et al., 2016a). Under this assumption, the lawn showed greater enrichment of $\delta^{15}\text{N}$ and $\delta^{18}\text{O}$ subsequent to nitrification, implying a greater fraction of NO_3^- loss to denitrification relative to the meadow in agreement with the denitrification potential assays. Trends in $\delta^{15}\text{N}$ of NO_3^- with depth in the lawn also corresponded with the denitrification potential assays: $\delta^{15}\text{N}$ of NO_3^- was greater in 0 – 5 cm soils, which had greater potential denitrification rates. Previous studies have similarly demonstrated greater

denitrification potential in surface than subsurface soil horizons (Groffman et al., 2002) and have reported high denitrification rates in lawns (Raciti et al., 2011). Both factors reflect the importance of plant C and N inputs (and potentially fertilizer additions) as controls on denitrification in surface soils, as opposed to O₂ diffusion limitation in the subsurface. However, if we had assessed relationships between $\delta^{18}\text{O}$ and $\delta^{15}\text{N}$ of NO₃⁻ at the lawn site alone without the context of the meadow samples with much lower denitrification rates, this conclusion would have been obscured. The meadow samples revealed the likely importance of fractionation during nitrification, and without accounting for this fractionation we would have had little isotopic evidence for denitrification at the lawn—even though denitrification potential assays and Fe(II) measurements strongly suggested it had occurred. This highlights a critical limitation in the use of NO₃⁻ isotopes to infer site-specific or watershed-scale patterns of denitrification, as recently implemented elsewhere.

Contrasting NO₃⁻ isotope compositions in soil extractions and lysimeter water

In contrast to the linear trend in the soil extractions, $\delta^{18}\text{O}$ and $\delta^{15}\text{N}$ values in soil lysimeter NO₃⁻ exhibited significant scatter, likely reflecting multiple fractionating processes and mixing with atmospheric NO₃⁻ that was enriched in ¹⁸O. The NO₃⁻ isotope disparities between lysimeters and soil extractions may also reflect the redox heterogeneity of terrestrial soils (Sexstone et al., 1985). Measurements of Fe(II)/Fe_{HCl} in soil extractions suggested the presence of reducing conditions in soil microsites, whereas the soil O₂ sensors indicated highly aerobic conditions at the scale of the bulk soil atmosphere in both sites (Table 1). Differences in dual isotope ($\delta^{18}\text{O}/\delta^{15}\text{N}$) slopes and $\delta^{15}\text{N}$ and $\delta^{18}\text{O}$ values between the soil extractions and the lysimeters support our hypothesis that soil extractions and lysimeter samples differ in their capacity to record ecosystem-scale N biogeochemical cycling via stable isotopes. A plausible

explanation for this pattern is that soil extractions sampled the anaerobic microsites inside soil aggregates where denitrification can occur (Parkin et al., 1987), whereas lysimeters largely reflected the transport of N that was nitrified in the aerobic macropore environment or in surface litter.

This distinction may be critical in interpreting patterns of denitrification at the watershed scale, where the NO_3^- isotopic composition of stream water is often assumed to integrate gross nitrification or denitrification across entire watersheds (Fang et al., 2015; Riha et al., 2014). Our data suggest that this assumption does not necessarily hold, given that relatively mobile lysimeter water and soil extractions from the same sites differed substantially in their NO_3^- isotope composition. Rather, as supported by recent syntheses of H_2O isotope dynamics, these samples may reflect two “water worlds”: poorly mobile water accessible to plants and microbes, and comparatively mobile water that dominates groundwater recharge and stream discharge (Evaristo et al., 2015; Good et al., 2015). Thus, stream or groundwater NO_3^- isotope composition may not necessarily reflect denitrification in surface soil microsites, a dominant zone of potential denitrification activity due to elevated inputs of C and N (Groffman et al., 2002).

Implications for interpreting $\delta^{15}\text{N}$ in models and environmental samples

Importantly, dual isotope trends in soil KCl extractable NO_3^- from both sites combined were consistent with denitrification isotope effects (Fig. 1) and were related to potential denitrification rates (Fig. 2) despite the fact that $\delta^{15}\text{N}$ values of NO_3^- were typically less than bulk soil $\delta^{15}\text{N}$. This finding has interesting implications for models that estimate denitrification at the ecosystem scale using isotopic measurements of NO_3^- (Billy et al., 2010; Fang et al., 2015). Our data suggest that substantial denitrification might occur even in situations where $\delta^{15}\text{N}$ values

of NO_3^- do not display substantial enrichment relative to N inputs or other ecosystem pools, due to the potentially large initial N isotope fractionation associated with nitrification. Thus, isotope models which assume that $\delta^{15}\text{N}$ of surface soil NO_3^- predominantly represents the product of nitrification (Fang et al., 2015) would tend to underestimate the relative importance of denitrification in the case where large fractionation effects of nitrification were partially counteracted by denitrification. In the latter study (ibid.), correlations between $\delta^{15}\text{N}$ and $\delta^{18}\text{O}$ of NO_3^- were not significant in surface soil KCl extractions, leading the authors to conclude that NO_3^- dynamics were spatially separated in these sites, with nitrification dominating in near-surface soils and denitrification prevailing in deeper soils.

The very weak linear trends between $\delta^{15}\text{N}$ and $\delta^{18}\text{O}$ we observed at the lawn site alone (as opposed to considering all samples together), combined with our process-level measurements, show that denitrification is not necessarily well recorded by site-specific trends in NO_3^- isotope composition in surface soils. Rather, $\delta^{15}\text{N}$ of NO_3^- showed a threshold relationship with potential denitrification rates and reducing conditions—strong trends at low rates that became a null relationship at higher rates. This may reflect closed-system kinetics where NO_3^- is mostly consumed via denitrification in soil microsites, leading to an under-expression of kinetic isotope effects as noted previously in both soils and sediments (Houlton et al., 2006; Sebilo et al., 2003). Thus, pairwise trends between $\delta^{15}\text{N}$ and $\delta^{18}\text{O}$ of NO_3^- and their relationships with potential denitrification only became strongly significant when considering a very broad gradient in redox variability and potential denitrification activity (which spanned three orders of magnitude among samples and sites, Figure 2). Moreover, our results are consistent with a recent global-scale analysis of soil $\delta^{15}\text{N}$, which found that much of the variability in bulk soil $\delta^{15}\text{N}$ previously attributed to denitrification might instead be explained by clay content and preferential retention

of microbially-processed organic matter (Craine et al., 2015). Differences in clay content between our sites (with loam and sandy loam texture, respectively) could contribute to the fact that bulk soil $\delta^{15}\text{N}$ did not reflect the large site differences in denitrification potential and $\delta^{15}\text{N}$ of soil extracted NO_3^- .

In summary, recent analytical and conceptual advances related to NO_3^- isotopes provide powerful opportunities for exploring controls on N sources and biogeochemical processing over multiple spatial scales (Fang et al., 2015; Houlton et al., 2006; Kendall et al., 2007; Michalski et al., 2004; Riha et al., 2014). We showed that surface soils characterized by denitrification at the microsite scale in a heterogeneous redox environment can exhibit NO_3^- isotope trends consistent with denitrification when examining samples exhibiting a broad range of potential denitrification rates. However, these patterns are highly dependent on spatial scale (i.e., comparisons among vs. within sites), sample type (soil extractions vs. lysimeter water), and assumptions about NH_4^+ isotope composition, nitrification isotope effects, and initial NO_3^- isotope composition prior to any denitrification. Thus, we suggest that NO_3^- isotope data should be interpreted with careful consideration of boundary conditions, sample types, and hydrologic connectivity between sampled pools before using them as parameter inputs or response variables in N cycling models.

Acknowledgements

We gratefully acknowledge field and lab assistance from Simone Jackson, Jillian Turner, Dave Eiriksson, Kendalynn Morris, and contributions from Suvankar Chakraborty, Gabe Bowen, and Jim Ehleringer in implementing the denitrifier method at SIRFER. This research was supported by NSF EPSCoR grant IIA 1208732 awarded to Utah State University, as part of the State of Utah Research Infrastructure Improvement Award, and by NSF grant DBI-1337947.

Any opinions, findings, and conclusions or recommendations expressed are those of the author(s) and do not necessarily reflect the views of the National Science Foundation.

References

Bai, E., Houlton, B.Z., 2009. Coupled isotopic and process-based modeling of gaseous nitrogen losses from tropical rain forests. *Global Biogeochemical Cycles* 23, GB2011. doi:10.1029/2008GB003361

Bell, M.D., Sickman, J.O., 2014. Correcting for background nitrate contamination in KCl-extracted samples during isotopic analysis of oxygen and nitrogen by the denitrifier method. *Rapid Communications in Mass Spectrometry* 28, 520–526. doi:10.1002/rcm.6824

Billy, C., Billen, G., Sebilo, M., Birgand, F., Tournebize, J., 2010. Nitrogen isotopic composition of leached nitrate and soil organic matter as an indicator of denitrification in a sloping drained agricultural plot and adjacent uncultivated riparian buffer strips. *Soil Biology and Biochemistry* 42, 108–117. doi:10.1016/j.soilbio.2009.09.026

Brooks, P.D., Grogan, P., Templer, P.H., Groffman, P., Öquist, M.G., Schimel, J., 2011. Carbon and nitrogen cycling in snow-covered environments. *Geography Compass* 5, 682–699. doi:10.1111/j.1749-8198.2011.00420.x

Brooks, P.D., Williams, M.W., 1999. Snowpack controls on nitrogen cycling and export in seasonally snow-covered catchments. *Hydrological Processes* 13, 2177–2190. doi:10.1002/(SICI)1099-1085(199910)13:14/15<2177::AID-HYP850>3.0.CO;2-V

Casciotti, K.L., Sigman, D.M., Hastings, M.G., Böhlke, J.K., Hilkert, A., 2002. Measurement of the oxygen isotopic composition of nitrate in seawater and freshwater using the denitrifier method. *Analytical Chemistry* 74, 4905–4912. doi:10.1021/ac020113w

471 Casciotti, K.L., Sigman, D.M., Ward, B.B., 2003. Linking diversity and stable isotope
 472 fractionation in ammonia-oxidizing bacteria. *Geomicrobiology Journal* 20, 335–353.
 473 Castellano, M.J., Lewis, D.B., Kaye, J.P., 2013. Response of soil nitrogen retention to the
 474 interactive effects of soil texture, hydrology, and organic matter. *Journal of Geophysical*
 475 *Research: Biogeosciences* 118, 280–290. doi:10.1002/jgrg.20015
 476 Chapelle, F.H., McMahon, P.B., Dubrovsky, N.M., Fujii, R.F., Oaksford, E.T., Vroblesky, D.A.,
 477 1995. Deducing the distribution of terminal electron-accepting processes in
 478 hydrologically diverse groundwater systems. *Water Resources Research* 31, 359–371.
 479 Cohen, M.J., Heffernan, J.B., Albertin, A., Martin, J.B., 2012. Inference of riverine nitrogen
 480 processing from longitudinal and diel variation in dual nitrate isotopes. *Journal of*
 481 *Geophysical Research: Biogeosciences* 117, G01021. doi:10.1029/2011JG001715
 482 Craine, J.M., Elmore, A.J., Wang, L., Augusto, L., Baisden, W.T., Brookshire, E.N.J., Cramer,
 483 M.D., Hasselquist, N.J., Hobbie, E.A., Kahmen, A., Koba, K., Kranabetter, J.M., Mack,
 484 M.C., Marin-Spiotta, E., Mayor, J.R., McLauchlan, K.K., Michelsen, A., Nardoto, G.B.,
 485 Oliveira, R.S., Perakis, S.S., Peri, P.L., Quesada, C.A., Richter, A., Schipper, L.A.,
 486 Stevenson, B.A., Turner, B.L., Viani, R.A.G., Wanek, W., Zeller, B., 2015. Convergence
 487 of soil nitrogen isotopes across global climate gradients. *Scientific Reports* 5, 8280.
 488 doi:10.1038/srep08280
 489 Dawson, T.E., Ehleringer, J.R., 1991. Streamside trees that do not use stream water. *Nature* 350,
 490 335–337. doi:10.1038/350335a0
 491 Evans, R.D., 2001. Physiological mechanisms influencing plant nitrogen isotope composition.
 492 *Trends in Plant Science* 6, 121–126. doi:10.1016/S1360-1385(01)01889-1

493 Evaristo, J., Jasechko, S., McDonnell, J.J., 2015. Global separation of plant transpiration from
 494 groundwater and streamflow. *Nature* 525, 91–94. doi:10.1038/nature14983
 495 Fang, Y., Koba, K., Makabe, A., Takahashi, C., Zhu, W., Hayashi, T., Hokari, A.A., Urakawa,
 496 R., Bai, E., Houlton, B.Z., Xi, D., Zhang, S., Matsushita, K., Tu, Y., Liu, D., Zhu, F.,
 497 Wang, Z., Zhou, G., Chen, D., Makita, T., Toda, H., Liu, X., Chen, Q., Zhang, D., Li, Y.,
 498 Yoh, M., 2015. Microbial denitrification dominates nitrate losses from forest ecosystems.
 499 *Proceedings of the National Academy of Sciences* 112, 1470–1474.
 500 doi:10.1073/pnas.1416776112
 501 Galloway, J.N., Aber, J.D., Erisman, J.W., Seitzinger, S.P., Howarth, R.W., Cowling, E.B.,
 502 Cosby, B.J., 2003. The nitrogen cascade. *BioScience* 53, 341–356. doi:10.1641/0006-
 503 3568(2003)053[0341:TNC]2.0.CO;2
 504 Good, S.P., Noone, D., Bowen, G., 2015. Hydrologic connectivity constrains partitioning of
 505 global terrestrial water fluxes. *Science* 349, 175–177. doi:10.1126/science.aaa5931
 506 Granger, J., Sigman, D.M., Lehmann, M.F., Tortell, P.D., 2008. Nitrogen and oxygen isotope
 507 fractionation during dissimilatory nitrate reduction by denitrifying bacteria. *Limnology*
 508 *and Oceanography* 53, 2533–2545.
 509 Granger, J., Sigman, D.M., Rohde, M.M., Maldonado, M.T., Tortell, P.D., 2010. N and O
 510 isotope effects during nitrate assimilation by unicellular prokaryotic and eukaryotic
 511 plankton cultures. *Geochimica et Cosmochimica Acta* 74, 1030–1040.
 512 doi:10.1016/j.gca.2009.10.044
 513 Groffman, P.M., 2012. Terrestrial denitrification: challenges and opportunities. *Ecological*
 514 *Processes* 1, 1–11.

515 Groffman, P.M., Boulware, N.J., Zipperer, W.C., Pouyat, R.V., Band, L.E., Colosimo, M.F.,
 516 2002. Soil nitrogen cycle processes in urban riparian zones. *Environmental Science &*
 517 *Technology* 36, 4547–4552. doi:10.1021/es020649z

518 Groffman, P.M., Holland, E.A., Myrold, D.D., Robertson, G.P., Zou, X., 1999. Denitrification,
 519 in: Robertson, G.P., Bledsoe, C.S., Coleman, D.C., Sollins, P. (Eds.), *Standard Soil*
 520 *Methods for Long-Term Ecological Research*. Oxford University Press, New York, pp.
 521 272–290.

522 Hall, S.J., McDowell, W.H., Silver, W.L., 2013. When wet gets wetter: Decoupling of moisture,
 523 redox biogeochemistry, and greenhouse gas fluxes in a humid tropical forest soil.
 524 *Ecosystems* 16, 576–589. doi:10.1007/s10021-012-9631-2

525 Hall S.J., Silver W.L. (2015) Reducing conditions, reactive metals, and their interactions can
 526 explain spatial patterns of surface soil carbon in a humid tropical forest. *Biogeochemistry*
 527 125:149–165. doi: 10.1007/s10533-015-0120-5

528 Hall, S.J., Weintraub, S.R., Eiriksson, D., Brooks, P.D., Baker, M.A., Bowen, G.J., Bowling,
 529 D.R., 2016a. Stream nitrogen inputs reflect groundwater across a snowmelt-dominated
 530 montane to urban watershed. *Environmental Science & Technology* 50, 1137–1146.
 531 doi:10.1021/acs.est.5b04805

532 Hall, S.J., Baker, M.A., Jones, S.B., Stark, J., Bowling, D.R., 2016b. Contrasting soil nitrogen
 533 dynamics across a montane meadow and urban lawn in a semi-arid watershed. *Urban*
 534 *Ecosystems* In press. doi:10.1007/s11252-016-0538-0

535 Holmes, R.M., McClelland, J.W., Sigman, D.M., Fry, B., Peterson, B.J., 1998. Measuring ^{15}N –
 536 NH_4^+ in marine, estuarine and fresh waters: An adaptation of the ammonia diffusion

537 method for samples with low ammonium concentrations. *Marine Chemistry* 60, 235–243.
 538 doi:10.1016/S0304-4203(97)00099-6
 539 Houlton, B.Z., Bai, E., 2009. Imprint of denitrifying bacteria on the global terrestrial biosphere.
 540 *Proceedings of the National Academy of Sciences* 106, 21713–21716.
 541 doi:10.1073/pnas.0912111106
 542 Houlton, B.Z., Sigman, D.M., Hedin, L.O., 2006. Isotopic evidence for large gaseous nitrogen
 543 losses from tropical rainforests. *Proceedings of the National Academy of Sciences* 103,
 544 8745–8750. doi:10.1073/pnas.0510185103
 545 Kendall, C., Elliott, E.M., Wankel, S.D., 2007. Tracing anthropogenic inputs of nitrogen to
 546 ecosystems, in: Michener, R., Lajtha, K. (Eds.), *Stable Isotopes in Ecology and*
 547 *Environmental Science*. Blackwell Publishing Ltd, pp. 375–449.
 548 Kool, D.M., Wrage, N., Oenema, O., Van Kessel, C., Van Groenigen, J.W., 2011. Oxygen
 549 exchange with water alters the oxygen isotopic signature of nitrate in soil ecosystems.
 550 *Soil Biology and Biochemistry* 43, 1180–1185. doi:10.1016/j.soilbio.2011.02.006
 551 Kulkarni, M.V., Groffman, P.M., Yavitt, J.B., 2008. Solving the global nitrogen problem: it's a
 552 gas! *Frontiers in Ecology and the Environment* 6, 199–206. doi:10.1890/060163
 553 Landon, M.K., Delin, G.N., Komor, S.C., Regan, C.P., 1999. Comparison of the stable-isotopic
 554 composition of soil water collected from suction lysimeters, wick samplers, and cores in
 555 a sandy unsaturated zone. *Journal of Hydrology* 224, 45–54. doi:10.1016/S0022-
 556 1694(99)00120-1
 557 Lehmann, M.F., Reichert, P., Bernasconi, S.M., Barbieri, A., McKenzie, J.A., 2003. Modelling
 558 nitrogen and oxygen isotope fractionation during denitrification in a lacustrine redox-

559 transition zone. *Geochimica et Cosmochimica Acta* 67, 2529–2542. doi:10.1016/S0016-
560 7037(03)00085-1

561 Mariotti, A., Germon, J.C., Hubert, P., Kaiser, P., Letolle, R., Tardieux, A., Tardieux, P., 1981.
562 Experimental determination of nitrogen kinetic isotope fractionation: Some principles;
563 illustration for the denitrification and nitrification processes. *Plant and Soil* 62, 413–430.
564 doi:10.1007/BF02374138

565 Mayer, B., Bollwerk, S.M., Mansfeldt, T., Hütter, B., Veizer, J., 2001. The oxygen isotope
566 composition of nitrate generated by nitrification in acid forest floors. *Geochimica et*
567 *Cosmochimica Acta* 65, 2743–2756. doi:10.1016/S0016-7037(01)00612-3

568 Michalski, G., Meixner, T., Fenn, M., Hernandez, L., Sirulnik, A., Allen, E., Thiemens, M., 2004.
569 Tracing atmospheric nitrate deposition in a complex semiarid ecosystem using $\Delta^{17}\text{O}$.
570 *Environmental Science & Technology* 38, 2175–2181. doi:10.1021/es034980+

571 Parkin, T., Starr, J., Meisinger, J., 1987. Influence of sample size on measurement of soil
572 denitrification. *Soil Science Society of America Journal* 51, 1492–1501.

573 Petersen, D.G., Blazewicz, S.J., Firestone, M., Herman, D.J., Turetsky, M., Waldrop, M., 2012.
574 Abundance of microbial genes associated with nitrogen cycling as indices of
575 biogeochemical process rates across a vegetation gradient in Alaska. *Environmental*
576 *Microbiology* 14, 993–1008. doi:10.1111/j.1462-2920.2011.02679.x

577 Raciti, S.M., Burgin, A.J., Groffman, P.M., Lewis, D.N., Fahey, T.J., 2011. Denitrification in
578 suburban lawn soils. *Journal of Environment Quality* 40, 1932. doi:10.2134/jeq2011.0107

579 Riha, K.M., Michalski, G., Gallo, E.L., Lohse, K.A., Brooks, P.D., Meixner, T., 2014. High
580 atmospheric nitrate inputs and nitrogen turnover in semi-arid urban catchments.
581 *Ecosystems* 17, 1309–1325. doi:10.1007/s10021-014-9797-x

582 Roach, W.J., Grimm, N.B., 2011. Denitrification mitigates N flux through the stream–floodplain
 583 complex of a desert city. *Ecological Applications* 21, 2618–2636. doi:10.1890/10-1613.1
 584 Schaetzl, R.J., Anderson, S., 2005. *Soils: Genesis and Geomorphology*. Cambridge University
 585 Press.
 586 Sebilo, M., Billen, G., Grably, M., Mariotti, A., 2003. Isotopic composition of nitrate-nitrogen as
 587 a marker of riparian and benthic denitrification at the scale of the whole Seine River
 588 system. *Biogeochemistry* 63, 35–51. doi:10.1023/A:1023362923881
 589 Sexstone, A., Revsbech, N., Parkin, T., Tiedje, J., 1985. Direct measurement of oxygen profiles
 590 and denitrification rates in soil aggregates. *Soil Science Society of America Journal* 49,
 591 645–651.
 592 Sigman, D.M., Granger, J., DiFiore, P.J., Lehmann, M.M., Ho, R., Cane, G., van Geen, A., 2005.
 593 Coupled nitrogen and oxygen isotope measurements of nitrate along the eastern North
 594 Pacific margin. *Global Biogeochemical Cycles* 19, GB4022. doi:10.1029/2005GB002458
 595 Wells, N.S., Baisden, W.T., Clough, T.J., 2015. Ammonia volatilisation is not the dominant
 596 factor in determining the soil nitrate isotopic composition of pasture systems. *Agriculture,*
 597 *Ecosystems & Environment* 199, 290–300. doi:10.1016/j.agee.2014.10.001
 598 Wexler, S.K., Goodale, C.L., McGuire, K.J., Bailey, S.W., Groffman, P.M., 2014. Isotopic
 599 signals of summer denitrification in a northern hardwood forested catchment.
 600 *Proceedings of the National Academy of Sciences* 111, 16413–16418.
 601 doi:10.1073/pnas.1404321111
 602 Yang, W.H., Teh, Y.A., Silver, W.L., 2011. A test of a field-based ¹⁵N–nitrous oxide pool
 603 dilution technique to measure gross N₂O production in soil. *Global Change Biology* 17,
 604 3577–3588. doi:10.1111/j.1365-2486.2011.02481.x

605 Zak, D.R., Groffman, P.M., Pregitzer, K.S., Christensen, S., Tiedje, J.M., 1990. The vernal dam:
606 plant-microbe competition for nitrogen in northern hardwood forests. Ecology 71, 651–
607 656. doi:10.2307/1940319
608

Table 1: Soil biogeochemical characteristics by depth for the lawn and meadow sites. Standard errors are in parentheses.

Site	Depth	pH	Bulk density (g cm ⁻³)	Soil δ ¹⁵ N	Soil N (%)	Soil N stock (kg N ha ⁻¹)	Fe(II) (μg g ⁻¹)	Fe(II)/ Fe _{HCl}	KCl- extractable NH ₄ ⁺ (μg g ⁻¹)	KCl- extractable NO ₃ ⁻ (μg g ⁻¹)	Lysimeter NO ₃ ⁻ -N (mg l ⁻¹)	Potential denitrification (μg N ₂ O-N g- h ⁻¹ at 25 °C)	Potential denitrification (μg N ₂ O-N g- h ⁻¹ at 4 °C)	Bulk soil O ₂ (%)
Lawn	0 - 5	7.5 (0.1)	0.86 (0.02)	3.3 (0.3)	0.36 (0.02)	1500 (200)	53 (7)	0.46 (0.08)	8.8 (1.5)	4.4 (1.8)	--	2955 (194)	406 (55)	--
	5 - 15	7.8 (0.1)	--	5.8 (0.1)	0.12 (0.01)	1800 (300)	23 (1)	0.32 (0.08)	2.1 (0.3)	1.3 (0.5)	0.67 (0.23)	709 (40)	35 (3)	19.6 (1.1)
Meadow	0 - 5	7.7 (0.1)	0.87 (0.02)	3.8 (0.1)	0.41 (0.02)	1800 (200)	7 (1)	0.04 (0.01)	2.4 (0.2)	2.5 (0.2)	--	465 (62)	25 (3)	--
	5 - 15	7.7 (0.1)	--	4.3 (0.1)	0.36 (0.01)	3100 (300)	8 (1)	0.03 (0)	3.9 (0.3)	2.9 (0.2)	--	217 (20)	11 (3)	20.7 (0.1)
	15 - 35	7.8 (0.1)	--	5.5 (0.1)	0.23 (0.01)	4000 (400)	7 (1)	0.03 (0)	3.6 (0.3)	1.1 (0.1)	0.24 (0.04)	65 (15)	3 (0)	--

Table 2: Nitrate isotope composition in soil KCl extractions and lysimeter samples from the lawn and meadow. Water $\delta^{18}\text{O}$ values from meadow lysimeters are also presented; these were very similar to precipitation $\delta^{18}\text{O}$ during the period of sampling (Hall et al., 2016b). Values in parentheses represent standard errors.

Site	Sample type	Sample size	$\text{NO}_3^- \delta^{15}\text{N}$ (‰)	$\text{NO}_3^- \delta^{18}\text{O}$ (‰)
Lawn	Lysimeter (NO_3^-)	15	-1.2 (1.7)	-9.5 (1.2)
Lawn	Soil extract (NO_3^-)	23	4.2 (1.2)	9.6 (2.4)
Meadow	Lysimeter (NO_3^-)	16	1.7 (0.5)	-12.5 (3.2)
Meadow	Soil extract (NO_3^-)	27	-9.9 (1.2)	-8.4 (1.2)
Meadow	Lysimeter (H_2O)	17	--	-17.7 (0.4)
Salt Lake City	Precipitation NO_3^-	8	2.3 (0.7)	81.9 (4.0)

Figure captions

Figure 1: a) Conceptual dual isotope plot ($\delta^{18}\text{O}$ and $\delta^{15}\text{N}$) showing measured variation of $\delta^{15}\text{N}$ of SOM, litter, and fertilizer as a vertical rectangle and measured variation of precipitation $\delta^{18}\text{O}$ as a horizontal rectangle. The predicted isotope composition of nitrified NO_3^- with complete expression of kinetic isotope effects on $\delta^{15}\text{N}$ is bounded by a black rectangle. This incorporates potential N fractionation during nitrification of an NH_4^+ source with $\delta^{15}\text{N}$ within the observed range of SOM, litter, and fertilizer, and $\text{NO}_3^- \delta^{18}\text{O}$ ranging from complete incorporation of soil water to a 1/3 contribution from atmospheric O_2 with $\delta^{18}\text{O} = 23.5$ ‰ (Kool et al., 2011; Mayer et al., 2001). The dotted line represents an illustrative trend of kinetic denitrification isotope effects with a $\delta^{18}\text{O}/\delta^{15}\text{N}$ slope of one, beginning at an arbitrary point in $\delta^{18}\text{O}/\delta^{15}\text{N}$ space. The vertical arrow indicates potential impacts of mixing with atmospheric NO_3^- enriched in $\delta^{18}\text{O}$. b)

Measurements of NO_3^- isotopes in soil KCl extractions (black symbols) and lysimeter water samples (open symbols). Triangles and circles represent the lawn and meadow sites, respectively. The dashed line represents a linear regression of $\delta^{18}\text{O}$ and $\delta^{15}\text{N}$ values in soil KCl extractions from both sites (slope = 1.04 ± 0.12 , $R^2 = 0.64$, $p < 0.0001$).

Figure 2: a) Relationship between $\delta^{15}\text{N}$ of NO_3^- in soil extractions and potential denitrification rate; the grey line represents a piecewise linear regression as described in the text. b)

Relationships between $\delta^{15}\text{N}$ of NO_3^- in soil extractions and the $\text{Fe(II)}/\text{Fe}_{\text{HCl}}$ ratio (a redox indicator, described in the text and Hall et al., 2015); the grey line represents a piecewise linear regression.

Figure 1:

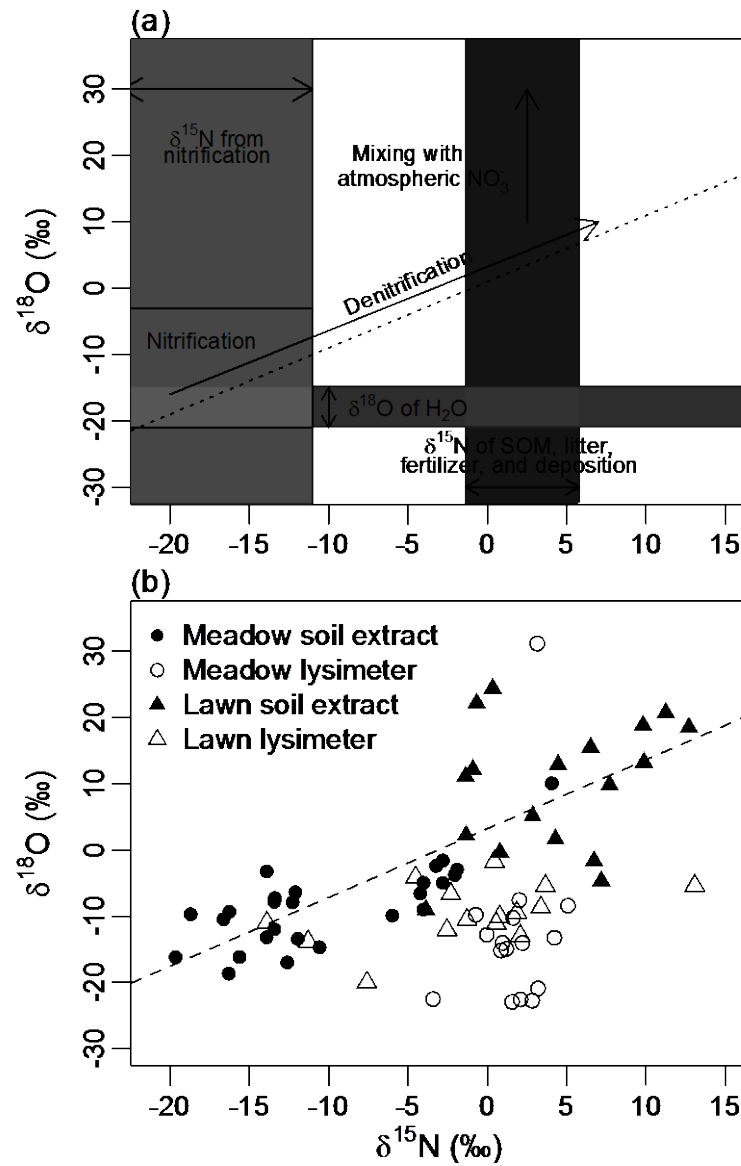


Figure 2:

